15th Triennial World Congress, Barcelona, Spain

STABILITY ANALYSIS OF FUZZY REACTIVE NAVIGATION

F. Cuesta and A. Ollero

Departamento de Ingeniería de Sistemas y Automática
Escuela Superior de Ingenieros
Camino de los Descubrimientos, 41092 Sevilla (Spain)
E-mail: {fede,aollero}@cartuja.us.es

Abstract: This paper presents stability analysis of fuzzy reactive navigation applied to the nonholonomic mobile robot ROMEO-3R. Reactive navigation approaches are emerging as an alternative to (or in combination with) planned schemes, but they usually present worse dynamic performance (oscillations are very common in these techniques). Influence of the own reactive navigation parameters (such as sensor range, computation time, control gains,...) in the stability of the system is analysed. Furthermore, stability conditions in terms of these parameters are also introduced. *Copyright © 2002 IFAC.*

Keywords: Mobile Robots, Reactive Navigation, Stability Analysis, Fuzzy Control.

1. INTRODUCTION

Planned navigation is very common in mobile robotics (Latombe, 1991). This approach is well suited to situations where the mobile robot has (or is able to build up) an accurate enough representation of the environment and also and an accurate position estimation. Then, high accuracy in path tracking can be achieved.

On the other hand, reactive navigation approaches have been proposed to deal with complex and uncertain environments where models are not available nor reliable. Furthermore, fuzzy logic has been widely applied to mobile robot control due to its inherent capabilities to deal with imprecise information and the flexibility of nonlinear control laws (Sugeno and Nishida, 1985; Saffiotti, 1997; Ollero *et al.*, 1999b; Song and Sheen, 2000; Cuesta *et al.*, 2002). However, reactive issues usually exhibit worse dynamic properties (such as oscillations) than the planned methods (Koren and Borenstein, 1991).

It should be pointed out that reactive navigation has a strong dependency on the sensed data, and, at the same time, the ability to perceive fast enough is very important in order to react properly. Furthermore, these elements play a significant role in the stability of the reactive navigation as will be shown in this paper. In this way, stability conditions taking into account the own reactive navigation parameters will be derived.

In the next section a brief description of the fuzzy reactive control is performed. In Section 3, stability of the fuzzy reactive navigation is analyzed. Thus, stability conditions in terms of the own reactive navigation parameters are obtained, making an easier task their qualitative interpretation. Section 4 presents some experiments devoted to validate the stability results and to show the influence of the time delays in the reactive navigation performance. The paper closes with the conclusions and references.

2. FUZZY REACTIVE NAVIGATION

In this section, a brief overview of the fuzzy reactive navigation technique under consideration is introduced (the method is fully explained by the authors in Cuesta *et al.* (2002)).

The perception technique used in this paper is an extension of the so-called *general perception vector* (Braunstingl *et al.*, 1995). This method aims at constructing a so-called general perception of the surroundings of the mobile robot from the measuring data provided by all the sensors. It is represented as a vector called general perception vector, which provides a fuzzy description of the environment. Special attention has been paid to take into account the sensorial limitations and the nonholonomic kinematic constraints of ROMEO-3R (see Fig.1) (Ollero *et al.*, 1999a).

Fig. 1: ROMEO-3R, mobile robot.

The distance measurement (d_s) of each ultrasonic sensor (u) (see Fig.2) is transformed into a virtual perception vector $\boldsymbol{p_i}$, and then all of them are combined yielding the general perception vector $\boldsymbol{p}$. The length of each vector is calculated in the range [0-1] by means of a perception function defined as (Cuesta *et al.*, 2002)

$$p_i = f(d_s, \varphi_i) = \mathrm{sat}_{0,1}\left(\frac{n d_m(1-\varepsilon\cos\varphi_i) - d_s(1-\varepsilon)}{(n-1)d_m(1-\varepsilon\cos\varphi_i)}\right) \quad (1)$$

where n is a positive number greater than 1, φ_i is the perception angle, and d_m is the minimum distance that can be perceived. Thus, an object detected in front of the vehicle, i.e. with a perception angle $\varphi_i = 0$, at the minimum distance d_m, will get the highest perception length ($p = 1$), while one detected at the maximum distance nd_m will get the lowest perception. Thus, an ellipsoidal perception area, as shown in Fig.3, is obtained, resulting in the curves of constant perception being ellipses of eccentricity ε ($0 < \varepsilon < 1$).

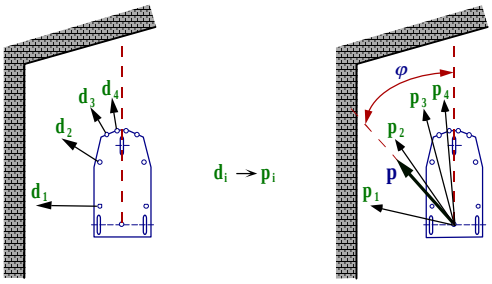

Fig. 2: General perception $\boldsymbol{p}$ of a mobile robot.

Perception vector can be considered by means of fuzzy logic using linguistic terms to describe the perception angle and the perception length as shown in Fig.3. Thus, a fuzzy description of the environment is obtained (e.g., the obstacle is located left-front and to a certain distance, between 0 and 1). This description of the environment, using the perception vector, can be used easily as input to a fuzzy controller in order to perform reactive navigation. Furthermore, it is also possible to compute different perception vectors and to use them to implement fuzzy controllers or behaviors which perform specific tasks. The combination of the different behaviors can be also easily done by means of fuzzy logic, thanks to the information provided by the perception vectors.

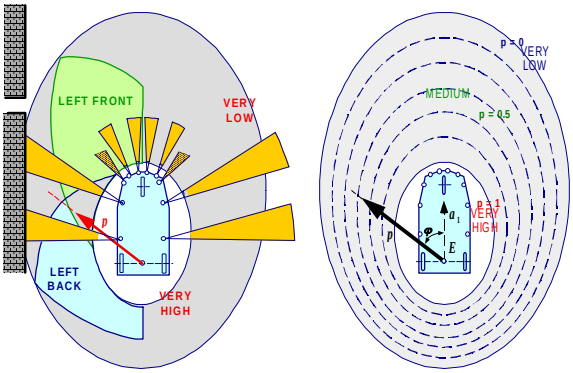

Fig. 3: Fuzzy perception

In case of *left wall following*, a *left hand perception vector* is built, yielding a left perception angle (φ_l), together with a left perception length (p_l). The goal of this behavior is to keep the left perception vector at a *medium* value and pointing to *left center*. This is achieved by fuzzy rules that use φ_l and p_l as inputs and the control commands for steering angle and linear velocity as outputs. The left wall following fuzzy logic controller is a conventional Mamdani one composed of fuzzy rules such as

IF φ_l IS LEFT_BACK AND p_l IS HIGH THEN MAKE *steer* CENTER;

Table 1 shows the whole rule base controlling the robot's direction of motion by means of the steering angle, where φ_l, for example, is described by the linguistic terms LF (Left_Front), LC (Left_Center), and LB (Left_Back).Fig.4 presents the results of a real experiment with ROMEO-3R. The robot performs a wall following mission with a maximum speed of 0.9 m/s.

Table 1. Rule base controlling steering angle.

$\varphi_l \backslash p_l$	VL	L	M	H	VH
LF	C	C	R	HR	HR
LC	HL	L	C	R	HR
LB	HL	L	C	C	R

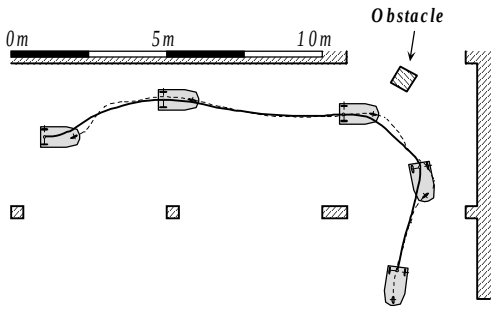

Fig. 4: ROMEO-3R navigating reactively.

3. STABILITY ANALYSIS OF REACTIVE NAVIGATION

3.1 Problem Statement

A stability analysis of general reactive navigation is rather complicated due to the nonlinear character of the elements involved. So, it could be seen like stability analysis of a vehicle (with its own kinematics and dynamic constraints), moving around an unknown environment that has to be perceived by using an arbitrary set of sensors placed at different locations, and with a control system (probably nonlinear) that guides the vehicle based on the system information.

For the sake of tractability, some assumptions have to be made for each element involved. Thus, from the point of view of the vehicle, a model considering its kinematics

$$\begin{aligned} \dot{x} &= -V\text{sen}\theta \\ \dot{y} &= V\cos\theta \\ \dot{\theta} &= V\gamma \end{aligned} \qquad (2)$$

(where $\gamma = (\tan\alpha)/l$ is the vehicle curvature, α is the steering angle, and l is the distance between axis) together with the dynamic of the steering system

$$\dot{\gamma} = -\frac{1}{\tau}(\gamma - u) \qquad (3)$$

will be used (τ is the time-constant of the steering system). Constant velocity V is also assumed.

On the other hand, the control problem will be to stabilize the vehicle to reactively follow a wall, large enough, at a given distance. Thus, environment perception will be performed using the perception vector and the control law is given by the Mamdani fuzzy controller introduced in Section 2. Fig.5 shows the nonlinear closed-loop under analysis.

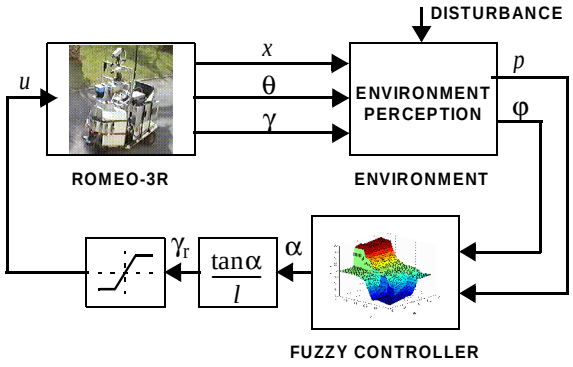

Fig. 5: Nonlinear closed-loop system.

3.2 Equilibrium points

Since it is a nonlinear system, the first step in the stability analysis will be to determine the equilibrium points. Then, by considering the model of the vehicle, the closed-loop equations are given by

$$\begin{aligned} \dot{x} &= -V\sin\theta \\ \dot{\theta} &= V\gamma \\ \dot{\gamma} &= -\frac{1}{\tau}(\gamma - \Phi(x, \theta, \gamma)) \end{aligned} \qquad (4)$$

where $\Phi(x, \theta, \gamma)$ is a nonlinear element including all the blocks out of the vehicle (that is, see Fig.5, fuzzy perception, fuzzy control, steering angle to curvature conversion, and control action saturation ($\pm 3.8\ \text{m}^{-1}$)).

Thus, system equilibria are given by the values $[x_e, \theta_e, \gamma_e]$, such that $[\dot{x}, \dot{\theta}, \dot{\gamma}] = 0$. In this way, system (4), becomes

$$\begin{aligned} 0 &= -V\sin\theta_e \\ 0 &= V\gamma_e \\ 0 &= -\frac{1}{\tau}(\gamma_e - \Phi(x_e, \theta_e, \gamma_e)) \end{aligned} \quad . \qquad (5)$$

From (5) it is easy to see that

$$\begin{aligned} \theta_e &= \pm k\pi, \qquad k = 0, 1, \ldots \\ \gamma_e &= 0 \end{aligned} \qquad (6)$$

and, therefore, third equation in (5) provides the following condition

$$\Phi(x_e, \pm k\pi, 0) = 0\,. \qquad (7)$$

In spite of the nonlinear character of (7), this equation can be easily solved by means of its graphical plot. So, for even values of k, i.e. ($k = \pm 2i$, $i = 0, 1, \ldots$), solutions of (7) are parametrized in x, by means of $\Phi(x_e, \pm 2i\pi, 0) = 0$, which graphical plot is shown in Fig.6 for $\varepsilon = 0.5$, $d_m = 1.3\text{m}$, $n = 3$ and $d_r = 1.3\text{m}$. Thus, for k even, the only solution corresponds to $x_e = 0$.

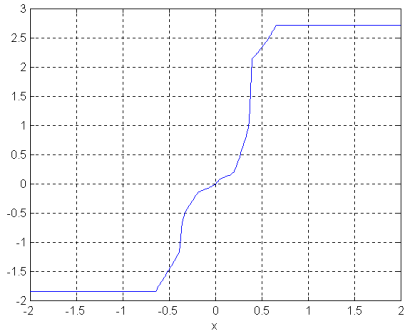

Fig. 6: Graphical plot of $\Phi(x_e, \pm k\pi, 0)$ with k even.

On the other hand, equation (7) evaluated for odd values of k, i.e. ($k = \pm(2i + 1)$, $i = 0, 1, \ldots$), yields 3.8 for any value of x (which corresponds with the maximum curvature).

Therefore, system equilibria are given by

$$[x_e, \theta_e, \gamma_e] = [0, \pm 2i\pi, 0],\ i = 0, 1, \ldots \qquad (8)$$

but only the origin will be considered ($i = 0$).

Local stability of the origin can be determined by means of the linearized system at the equilibrium point. Two cases will be considered, depending on the existence, or not, of time delays in the system.

3.3 System without time delays

If no delays are considered in the system, the linearized system can be obtained form the Jacobian of (4), yielding

$$\begin{bmatrix} \dot{x} \\ \dot{\theta} \\ \dot{\gamma} \end{bmatrix} = \begin{bmatrix} 0 & -V & 0 \\ 0 & 0 & V \\ \frac{\beta_1}{\tau} & \frac{\beta_2}{\tau} & \frac{-1}{\tau} \end{bmatrix} \begin{bmatrix} x \\ \theta \\ \gamma \end{bmatrix} \tag{9}$$

where $\beta_1 = \frac{\partial}{\partial x}\Phi(x, \theta)$ and $\beta_2 = \frac{\partial}{\partial \theta}\Phi(x, \theta)$.

Stability of (9), is given by its characteristic polynomial

$$P(s) = \det[sI - J] = \det\begin{bmatrix} s & V & 0 \\ 0 & s & -V \\ \frac{-\beta_1}{\tau} & \frac{-\beta_2}{\tau} & s + \frac{1}{\tau} \end{bmatrix} \tag{10}$$
$$= s^3 + \frac{1}{\tau}s^2 - \frac{\beta_2}{\tau}Vs + \frac{\beta_1}{\tau}V^2 = 0$$

Then, by means of the Routh Hurwitz criteria, the following necessary and sufficient conditions for the local stability of the origin can be derived:

$$\tau > 0, \beta_2 < 0, \beta_1 > 0$$
$$\beta_1 < -\frac{\beta_2}{V\tau} \tag{11}$$

3.4 System with time delays

Nevertheless, time delays exists in reactive navigation (these delays arises from different sources: sensor readings, computation of control action,...), and, therefore, they can not be neglected. So, by considering a time delay T, system (4) becomes

$$\begin{aligned} \dot{x} &= -V\sin\theta(t) \\ \dot{\theta} &= V\gamma(t) \\ \dot{\gamma} &= -\frac{1}{\tau}(\gamma(t) - \Phi(x(t-T), \theta(t-T), \gamma(t-T))) \end{aligned} \tag{12}$$

and the linearized system is

$$\begin{bmatrix} \dot{x} \\ \dot{\theta} \\ \dot{\gamma} \end{bmatrix} = J \begin{bmatrix} x(t) \\ \theta(t) \\ \gamma(t) \end{bmatrix} + J_T \begin{bmatrix} x(t-T) \\ \theta(t-T) \\ \gamma(t-T) \end{bmatrix} \tag{13}$$

where the corresponding Jacobians are

$$J = \begin{bmatrix} 0 & -V & 0 \\ 0 & 0 & V \\ 0 & 0 & -\frac{1}{\tau} \end{bmatrix} \qquad J_T = \begin{bmatrix} 0 & 0 & 0 \\ 0 & 0 & 0 \\ \frac{\beta_1}{\tau} & \frac{\beta_2}{\tau} & 0 \end{bmatrix} \tag{14}$$

Stability of the equilibrium point can be analyzed by means of its characteristic quasi-polynomial

$$\begin{aligned} Q(s) &= \det[sI - J - J_T e^{-sT}] \\ &= \det\begin{bmatrix} s & -V & 0 \\ 0 & s & V \\ \frac{-\beta_1}{\tau}e^{-sT} & \frac{-\beta_2}{\tau}e^{-sT} & s + \frac{1}{\tau} \end{bmatrix} \\ &= s^3 + \frac{1}{\tau}s^2 + \left(-\frac{\beta_2}{\tau}Vs + \frac{\beta_1}{\tau}V^2\right)e^{-sT} \end{aligned} \tag{15}$$

It can be shown that the condition for the asymptotic stability of solutions of linear equations with delayed arguments is that the real parts of all roots of the characteristic quasi-polynomial be negative. Then, applying stability condition $Q(j\omega) = 0$ to (15), and taking into account that $e^{-j\omega T} = \cos\omega T - j\sin\omega T$, it is obtained that

$$\begin{aligned} Q(j\omega) &= -j\omega^3 - \frac{\omega^2}{\tau} \\ &+ \left(-\frac{\beta_2}{\tau}Vj\omega + \frac{\beta_1}{\tau}V^2\right)(\cos\omega T - j\sin\omega T) = 0 \end{aligned} \tag{16}$$

from where it is easy to obtain two equations giving the stability limits

$$\begin{aligned} -\frac{\omega^2}{\tau} + \frac{\beta_1}{\tau}V^2\cos\omega T - \frac{\beta_2}{\tau}V\omega\sin\omega T &= 0 \\ -\omega^3 - \frac{\beta_1}{\tau}V^2\sin\omega T - \frac{\beta_2}{\tau}V\omega\cos\omega T &= 0 \end{aligned} \tag{17}$$

Furthermore, making a change of variable $\omega T = \psi$, and some algebraic operations in (17), the following conditions on β_1 and β_2 can also be obtained

$$\beta_1 = -\frac{\psi^2(-T\cos\psi + \tau\psi\sin\psi)}{V^2T^3}, \tag{18}$$

$$\beta_2 = -\frac{\psi(T\sin\psi + \tau\psi\cos\psi)}{VT^2} \tag{19}$$

In this way, is easy to see that as the velocity or the time delay grows, the maximum allowable values for the gains in the control action (β_1 and β_2) decrease. This result is agree with one could expect. In fact, it is well known that time delays reduce the gain margin of a system, and, on the other hand, a hard turn while driving at high speed could bring the vehicle out of control and, therefore, the control action, i.e. steering action, should be smoother.

3.5 *Relation with the parameters of reactive navigation*

Finally, in order to better understand the previous stability results, they will be recalled in terms of the own reactive navigation parameters. To do that, firstly the fuzzy controller will be approximated by its partial linearization at the origin, yielding that the control law is approximately:

$$\Phi(x,\theta) = \Phi(p,\varphi) = -k_1(p_r - p) - k_2(\varphi_r - \varphi) \quad (20)$$

where k_1 is given in m^{-1}, and k_2 in $rad^{-1}m^{-1}$.

Assuming that the system is working close to the equilibrium, perception function will not saturate and, therefore, $p \in (0,1)$ will be given by

$$p = \frac{nd_m(1-\varepsilon) - d(1-\varepsilon\cos\varphi)}{(n-1)d_m(1-\varepsilon)}. \quad (21)$$

Substituting (21) in (20), together with $\varphi = -\theta + \frac{\pi}{2}$ and $d = x + d_r$, yields

$$\begin{aligned}\Phi(x,\theta) = {} & -k_1\left(p_r - \frac{nd_m(1-\varepsilon) - d_r}{(n-1)d_m(1-\varepsilon)}\right) \\ & - \frac{k_1}{(n-1)d_m(1-\varepsilon)}x + \frac{k_1\varepsilon\cos\left(-\theta+\frac{\pi}{2}\right)}{(n-1)d_m(1-\varepsilon)}x \\ & + \frac{k_1\varepsilon d_r\cos\left(-\theta+\frac{\pi}{2}\right)}{(n-1)d_m(1-\varepsilon)} - k_2\left(\varphi_r - \frac{\pi}{2}\right) - k_2\theta\end{aligned} \quad (22)$$

Furthermore, since $p_r = \frac{nd_m(1-\varepsilon) - d_r}{(n-1)d_m(1-\varepsilon)}$, $\varphi_r = \frac{\pi}{2}$, and $\cos\left(-\theta+\frac{\pi}{2}\right) = \sin\theta$, it is obtained that

$$\begin{aligned}\Phi(x,\theta) = {} & -\frac{k_1}{(n-1)d_m(1-\varepsilon)}x + \\ & + \frac{k_1\varepsilon\sin\theta}{(n-1)d_m(1-\varepsilon)}x + \frac{k_1\varepsilon d_r\sin\theta}{(n-1)d_m(1-\varepsilon)} - k_2\theta\end{aligned} \quad (23)$$

where can be appreciated the strong nonlinear dependency with respect to x and θ.

Thus, from (23), the values for β_1 and β_2 can be obtained as

$$\begin{aligned}\beta_1 &= \frac{\partial}{\partial x}\Phi(x,\theta)\Big|_0 = \frac{-k_1}{(n-1)d_m(1-\varepsilon)} \\ \beta_2 &= \frac{\partial}{\partial\theta}\Phi(x,\theta)\Big|_0 = \frac{k_1\varepsilon d_r}{(n-1)d_m(1-\varepsilon)} - k_2\end{aligned} \quad (24)$$

Again, a qualitative interpretation of (24) is straightforward. In this way, for instance, the gain k_1 could be large as the sensor range, $(n-1)d_m$, becomes larger, and vice versa, a smaller sensorial capacity will imply a lower control action. On the other hand, recalling stability conditions (11) in terms of k_1 and k_2, it is obtained that

$$\begin{aligned}& k_1 < 0 \\ & \frac{-k_1(V\tau - \varepsilon d_r)}{(n-1)d_m(1-\varepsilon)} < k_2 \\ & V \le \frac{1}{\tau}\left(\varepsilon d_r + \frac{k_2}{|k_1|}(n-1)d_m(1-\varepsilon)\right)\end{aligned} \quad (25)$$

where can be observed that the ellipsoidal perception function ($\varepsilon \neq 0$) allows the system to be stable even for some negative values of k_2. Also, can be seen that, for a given controller, the maximum velocity will be higher as the sensor range grows, as one could expect. Similar conclusions can be drawn from system (18)-(19).

4. SIMULATION EXPERIMENTS

This section is devoted to validate the stability conditions derived in the previous section. Simulations will be used for the sake of repeatability. To that end, parameters from the actual fuzzy control system of ROMEO-3R mobile robot will be used, namely, the perception parameters are $\varepsilon = 0.5$, $d_m = 1.3\text{m}$, $n = 3$ and $d_r = 1.3\text{m}$; the time delay is $T = 0.1s$; and from the fuzzy controller: $\beta_1 = 0.824$ and $\beta_2 = -0.681$ (i.e., $k_1 = -1.358$ and $k_2 = 0.723$ from (24)). Fig.7 shows a simulation experiment at $V = 0.5m/s$, with an equivalent behavior to the real experiment with ROMEO-3R shown in Fig.4, performing a stable navigation as it was expected.

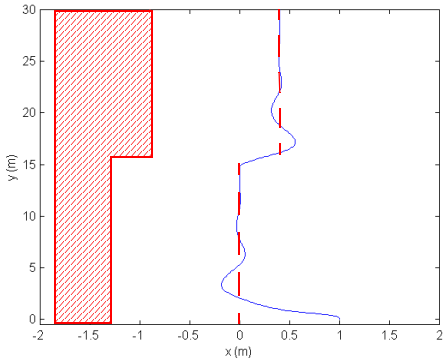

Fig. 7: ROMEO-3R navigating at V=0.5 m/s, T=0.1s.

In the following stability conditions will be used to show the influence of time delay in the navigation and to compute the maximum allowable stable velocity.

So, by keeping the perception and controller parameters, the maximum stable velocity with $T = 0.1s$, can be obtained by solving equations (18)-(19). This can be easily accomplished by means of their graphic representation, as shown in Fig.8. From this figure, the maximum stable velocity is approximately $V \approx 2.104m/s$, at which the vehicle will navigate showing oscillations at a frequency $\omega \approx 2.04\text{rad/s}$ (i.e, a period of 3.07s, approximately). This result can be verified by showing the vehicle

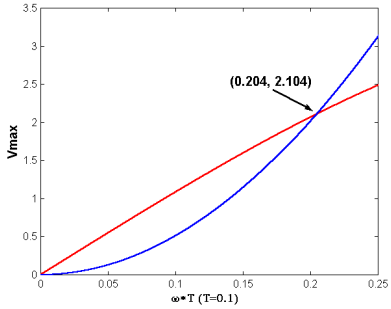

Fig. 8: Graphical plot of V from (18) (red), and (19) (blue), with T=0.1s.

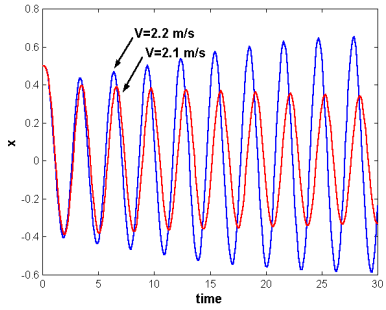

Fig. 9: Stable vehicle response at V=2.1m/s (red), and unstable at V=2.2 m/s (blue), with T=0.1s.

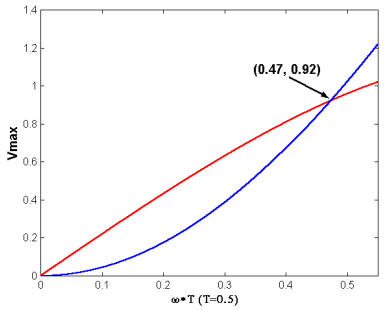

Fig. 10: Graphical plot of V from (18) (red), and (19) (blue), with T=0.5s.

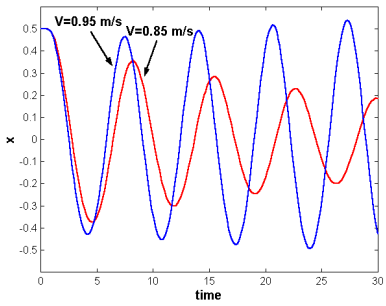

Fig. 11: Stable vehicle response at V=0.85m/s (red), and unstable at V=0.95 m/s (blue), with T=0.5s.

behavior navigating at velocities below and above of this limit, as shown in Fig.9, where a stable and an unstable oscillatory behavior are obtained, respectively.

Similarly, influence of the time delay can be also shown. So, solving equations (18)-(19) with a larger time delay ($T = 0.5s$), the maximum stable velocity becomes drastically reduced to $V \approx 0.92$m/s ($\omega \approx 0.94$rad/s), as shown in Fig.10 and Fig.11.

5. CONCLUSIONS

Reactive navigation approaches are emerging as an alternative to (or in combination with) planned schemes. However, they usually present worse dynamic performance, such as oscillations. On the other hand, reactive techniques have a strong dependency on the sensed information and demand fast response in order to properly react to the environment. In this paper, stability of reactive navigation has been analysed. Stability conditions, in terms of the own reactive navigation parameters (such as sensor range, computation time, control gains,...) have been obtained. Furthermore, influence of the time delay in the reactive navigation performance has been also pointed out by means of experiments.

Acknowledgment:

This work has been supported by CYCIT under project TAP99-0926-C04-01.

6. REFERENCES

Braunstingl, R., P. Sanz, J.M. Ezkerra (1995), Fuzzy logic wall following of a mobile robot based on the concept of general perception, *7th Int. Conf. on Advanced Robotics*, Vol 1, Spain, 367-376.

Cuesta, F., A. Ollero, B.C. Arrue and R. Braunstingl (2002). Intelligent control of nonholonomic mobile robots with fuzzy perception. *Fuzzy Sets and Systems*. To appear.

Koren, Y. and J. Borenstein (1991), Potential Field Methods and Their Inherent Limitations for Mobile Robot Navigation. *Proc. of the IEEE Int. Conf. on Robotics and Autom.* pp. 1398-1404.

Latombe**,** J.C. (1991). *Robot motion Planning.* Kluwer Academic Publishers, pag.. 424-425.

Ollero, A., B.C. Arrue, J. Ferruz, G. Heredia, F. Cuesta, F. López-Pichaco, C. Nogales (1999a), Control and perception components for autonomous vehicle guidance. Application to the romeo vehicles, *Control Engineering Practice*, 07 10 1291-1299.

Ollero, A., G. Ulivi, F. Cuesta (1999b), Fuzzy logic applications in mobile robotics, in: *Fuzzy Algorithms for Control*. Kluwer Academic Publishers, Boston, Chapter 11 301-324.

Saffiotti, A. (1997), Fuzzy logic in autonomous robot navigation: a case study, *Soft Computing* 1 4 180.

Song, K-T., and L-H. Sheen (2000), Heuristic fuzzy-neuro network and its application to reactive navigation of a mobile robot, *Fuzzy Sets and Systems*, 110 3 331-340.

Sugeno, M., and M. Nishida (1985), Fuzzy control of model car, *Fuzzy Sets and Systems* 16, 103-113.